**Research Article**

Investigation on the Growth and Characterization of Novel Creatininium malate Single Crystal

S. Mathuri[1], M. Kayalvizhi[2], G. Vasuki[2*], R. Ramesh Babu[3], K. Ramamurthi[1], A. Crochet[4], K. M. Fromm[5]

[1]Crystal Growth and Thin film Laboratory, Department of Physics and Nanotechnology, Faculty of Engineering and Technology SRM University, Kattankulathur – 603 203, Kancheepuram Dt, India
[2]Department of Physics, Kunthavai Naacchiyar Government Arts College (W) Autonomous, Thanjavur – 613 007, India
[3]Crystal Growth and Thin Film Laboratory, School of Physics, Bharathidasan University, Tiruchirappalli – 620 004, India
[4]FriMat, Fribourg Center for Nanaomaterials, University of Fribourg, Chemin du musée, 6, CH-1700 Fribourg, Switzerland
[5]Departement of Chemistry, University of Fribourg, Chemin du musée, 9, CH-1700 Fribourg, Switzerland

Abstract

A novel single crystal of creatininium malate was grown from aqueous solution by slow evaporation technique at room temperature. Single crystal X-ray diffraction analysis revealed that the crystal belongs to a centrosymmetric system with space group $P2_1/c$. The FT-IR spectrum was recorded to confirm the functional groups present in the grown crystal. The dielectric property of the grown crystal was studied as a function of frequency in the range of 50Hz to 1MHz at different temperatures. Creatininium malate crystals possess a high dielectric constant at lower frequencies. The mechanical strength of the crystal was estimated using Vickers microhardness tester. The thermal stability of the crystal was studied by thermogravimetric and differential thermal analyses.

Keywords: Crystal growth, Single crystal XRD, Powder X-ray diffraction, Dielectric properties, Mechanical properties
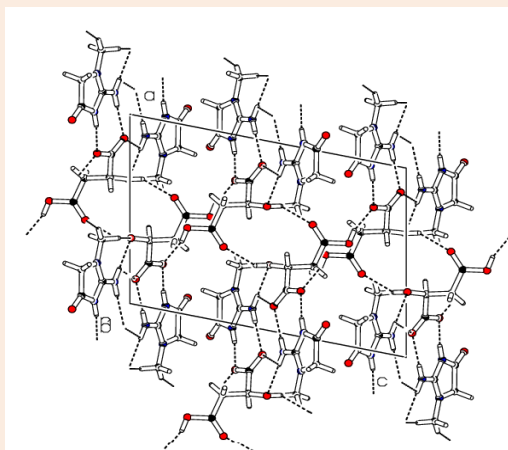
*Correspondence
Dr. G. Vasuki,
Email: vasuki.arasi@yahoo.com

Introduction

Materials with high nonlinear optical (NLO) efficiency find applications in the areas of optical communication, signal processing, sensing, higher harmonics generation, amplitude and phase modulation and laser technology [1-3]. Organic materials with π conjugate systems possess a wide range of optical transmittance, high laser damage threshold, fast optical response time and a wide phase matching angle when compared to that of the inorganic counterparts [4-6]. Organic molecules consisting of guest-host complexes have become effective NLO materials due to the anisotropic acentric crystalline framework of such crystals [7].

A proton transfer between carboxylic acids and Lewis bases provides considerable structural stability to the molecules and creates more hydrogen-bonding in the molecular association [8]. Over the last three decades there has been increasing number of reports on proton transfer compounds. Creatinine is a breakdown product of creatine phosphate during metabolic activity in living bodies [9]. Functional groups present in the creatinine molecule establish hydrogen bonding with other molecules. As creatinine acts as a proton acceptor in the proton transfer compounds, Smith and White [10] investigated on the synthesis of proton transfer compounds such as nitrobenzoic acids, 3,5 – dinitrosalicyclic acid, 5 – nitrosalicyclic acid, 3,5 – dinitrobenzoic acid and pyrazine- 2, 3 - dicarboxylic acid and also solved the crystal structure for creatinine with pyrazine - 2, 3 - dicarboxylic acid. Moghimi et al., [11] synthesized creatinine compound with 2, 6 - pyridinedicarboxy acid and studied the role of proton acceptor structure

of the resulting proton transfer compound. Further Moghimi et al., [12] demonstrated the generation of self-assembled supramolecular layers via proton transfer process for the pyridinium-2, 6-bis (monothiocarboxylate) and creatininium ion pair.

Bahadur et al., [13] determined the crystal structure of creatininium hydrogen oxalate monohydrate and studied the coordination chemistry between creatinine and oxalic acid. The crystal structure of creatininium benzoate was determined by Bahadur et al., [14]. The crystal structure and coordination chemistry of creatinine with maleic and creatinine with cinnamic acid were reported by Ali [15, 16]. Creatinine consists of both imino and amino tautomeric forms and possesses several substituents and functional groups, e.g CH_3, CH_2, NH_2 and C=O. Hence, based on the nature of metal ions and the reaction conditions, creatinine coordinates with metal ions [17]. Creatinine complexes with transition metal ions of Zn, Cd and Hg were reported by Muralidharan et al., [18]. Bayrak and Bayari [19] carried out DFT studies of the creatinine complex with transition metals (Zn, Cd and Hg). The complexation of creatinine with different metal ions (Pt, Pd, Ni and Cu) was reported by several authors [17, 20, 21].

DL-Malic acid is an organic material, which crystallizes in combination with other materials. The crystal structure of anilinium monohydrogen DL-malate was reported by Perpetuo and Janczak [22]. DL-Malic acid combines with ammonia solution and gives ammonium malate single crystal [23]. DL-Malic acid with boric acid and rubidium carbonate yields a potential semiorganic NLO material of rubidium bis-DL-malato borate [24]. DL-malic acid doped ammonium dihydrogen phosphate (ADP) crystal shows enhanced optical, mechanical and dielectric properties [25]. DL-malic acid and L-alanine produce L-alanine DL-malic acid single crystal [26].

In this work, we investigated the combination of malic acid with creatinine to learn if NLO materials can be produced. The synthesis, crystal growth, single crystal X-ray diffraction, powder X-ray diffraction, mechanical, dielectric and thermal properties of creatininium malate single crystals are reported for the first time.

Experimental procedure

Synthesis and growth of creatininium malate single crystal

Creatininium malate was synthesized from the aqueous solution of creatinine and DL-Malic acid taken in stoichiometric ratio. The chemical reaction between creatinine and DL-Malic acid yields the creatininium malate salt as given below:

$$C_4H_7N_3O + C_4H_6O_5 \rightarrow C_4H_8N_3O^+ \ C_4H_5O_5^-$$
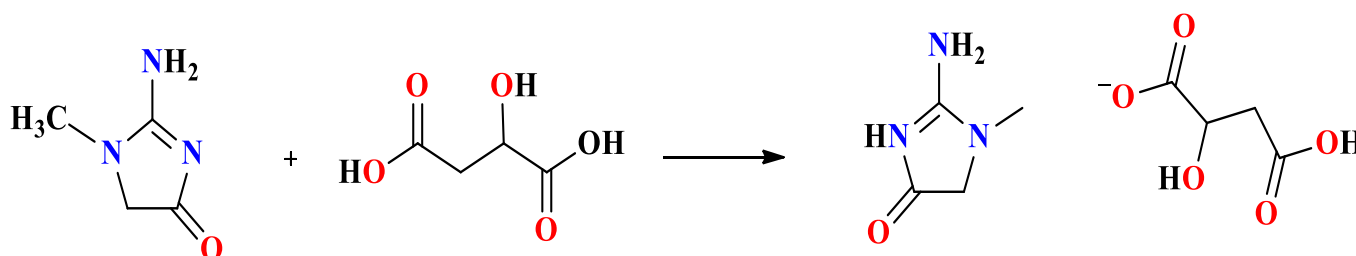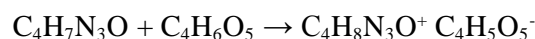
An aqueous solution of creatininium malate salt was prepared according to its solubility and the solution was stirred continuously at room temperature using a magnetic stirrer to obtain a homogeneous solution. The purity of the salt was improved by a repeated recrystallization process using double distilled water. The so-prepared solution of the recrystallized salt was filtered and taken in a beaker which was covered by parafilm to avoid contamination and to control the evaporation of the solvent. The solvent was allowed to evaporate slowly at room temperature which yielded well defined creatininium malate single crystals of 4x5x3 mm^3 size in a growth period of about 60 days. (**Figure 1**) shows the photograph of the as-grown crystals of creatininium malate.
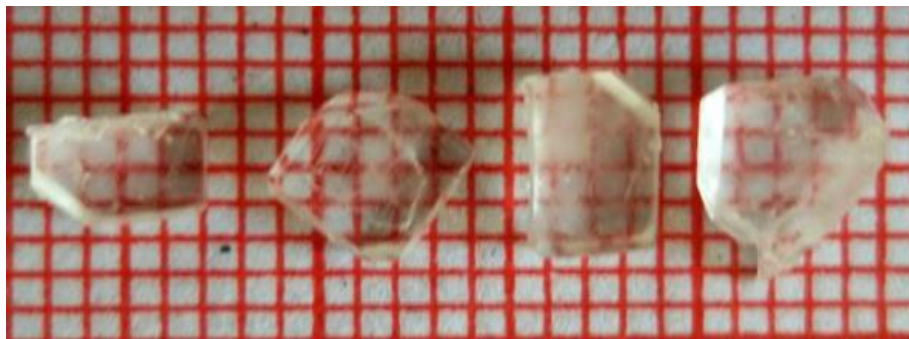
Figure 1

Characterization

The grown crystal was subjected to single crystal X-ray diffraction (XRD) studies using STOE IPDS 2 diffractometer to identify the crystal structure. A Fourier transform infrared (FTIR) spectrum was recorded using the FT-IR-Shimadzu IR Affinity 1 spectrometer in the range of 400-4000 cm^{-1}. The dielectric property of the crystal was measured by HIOKI 3532-50 LCR HITESTER impedance meter for different frequencies at various temperatures. Thermal analyses of the grown crystal were carried out using a thermal analyzer SDT Q600 V20.9 between 25°C and 300°C at a heating rate of 10 °C/min in nitrogen atmosphere. The mechanical properties of the grown crystal were studied by Vickers microhardness instrument Matsuzawa Hibiki model mmT X7.

Result and discussion

Single crystal X-ray diffraction analysis

A suitable single crystal of creatininium malate was selected and subjected to single crystal X-ray diffraction studies. The intensity data of the title compound was collected at 200K using MoK$_\alpha$ graphite monochromatic radiation of wavelength λ = 0.7107Å. The molecular structure of the crystal ($C_4H_8N_3O^+ C_4H_5O_5^-$) was refined by the least squares method using anisotropic thermal parameters:

R = 0.029%. The compound crystallizes in the monoclinic crystal system of space group P2$_1$/c. The calculated unit cell parameter values are *a = 10.9525(6) Å, b = 6.6327(4) Å, c = 15.1609(9) Å, β = 101.873(5) °, V = 1077.80(11) Å³ and Z = 4.*

The asymmetric unit of the title compound (I) contains one creatininium cation and one DL-malate anion. A single proton transfer occurred from one of the two carboxylic acid functional groups to the endocyclic imine N atom of creatinine. This results in an increase in the C7-N3 bond distance [1.3638(15) Å] and a decrease of C7 = N2 [1.3011(16) Å] when compared with the corresponding values of the neutral creatinine molecule 1.349(2) and 1.320(3) Å, respectively [10]. The creatininium malate crystal data and structural refinement parameters are presented in **(Table 1)**. Fractional atomic coordinates and isotropic or equivalent isotropic displacement factors for non-hydrogen atoms are presented in **(Table 2)**. The molecular structure of the title compound is shown with atom numbering and displacement ellipsoids drawn at the 50% probability level in **(Figure 2)**. The cations and anions in the packing are linked into ion pairs **(Figure 3)** via N-H…O hydrogen bonds (Table 3) with the formation of an R$_2^2$[8] motif [27]. The anions in the packing are linked into ion pairs **(Figure 4)** via O-H…O hydrogen bonds (Table 3) with the formation of an R$_2^2$ [12] motif. Other N-H…O hydrogen bonds (Table 3) link these ion pairs into zig zag chains running along the *b*-axis. For the title compound data collection and cell refinement were done using the computer program X-Area [28] and data reduction was done by using X-RED32 [28]. The structure of the title

compound was solved by direct methods using the computer program SHELXS-97 [29] and refined using SHELXL-97 [29]. The molecular graphics were done using the computer programs ORTEP-3 [30], Mercury [31] and PLATON [32].

Table 1

Empirical formula	C8 H13 N3 O6
Formula weight	247.21
Temperature	200(2) K
Wavelength	0.71073 Å
Crystal system	Monoclinic
Space group	P 21/c
Unit cell dimensions	a = 10.9525(6) Å α= 90°.
	b = 6.6327(4) Å β= 101.873(5)°.
	c = 15.1609(9) Å γ = 90°.
Volume	077.80(11) Å3
Z	4
Density (calculated)	1.524 Mg/m3
Absorption coefficient	0.131 mm-1
F(000)	520
Crystal size	0.450 x 0.343 x 0.200 mm3
Theta range for data collection	1.90 to 25.64°.
Index ranges	-13<=h<=13, -7<=k<=8, -18<=l<=18
Reflections collected	16245
Independent reflections	2033 [R(int) = 0.0793]
Completeness to theta = 25.64°	99.8 %
Absorption correction	None
Refinement method	Full-matrix least-squares on F2
Data / restraints / parameters	2033 / 0 / 170 Final R indices [I>2sigma(I)]
Goodness-of-fit on F2	1.043
Final R indices [I>2sigma(I)]	R1 = 0.0290, wR2 = 0.0737
R indices (all data)	R1 = 0.0346, wR2 = 0.0764
Largest diff. peak and hole	0.166 and -0.236 e.Å-3

Table 2

	x	y	z	U(eq)
O(1)	0.13425(7)	0.86732(14)	0.02075(6)	0.0275(2)
O(2)	0.24149(8)	0.64915(15)	0.11837(6)	0.0313(2)
O(3)	0.34591(8)	1.06919(14)	0.00384(6)	0.0287(2)
O(4)	0.54199 (8)	1.06752 (16)	0.29175 (6)	0.0343 (2)
O(5)	0.60426 (8)	1.04430 (15)	0.16148 (6)	0.0331 (2)
O(6)	−0.08999 (9)	0.67899 (16)	0.29093 (7)	0.0405 (3)
N(1)	0.17973 (9)	0.95187 (15)	0.38040 (7)	0.0234 (2)
N(2)	0.09812 (11)	1.23213 (17)	0.44312 (7)	0.0278 (2)
N(3)	−0.02406 (10)	0.96775 (16)	0.37034 (7)	0.0247 (2)
C(1)	0.23204 (10)	0.80587 (19)	0.06812 (7)	0.0222 (3)
C(2)	0.35436 (10)	0.92249 (19)	0.07258 (7)	0.0221 (3)
C(3)	0.38482 (11)	1.0285 (2)	0.16362 (8)	0.0271 (3)

C(4)	0.52166 (11)	1.04707 (18)	0.20412 (8)	0.0240 (3)
C(5)	−0.00832 (11)	0.7941 (2)	0.32486 (8)	0.0271 (3)
C(6)	0.12954 (11)	0.7791 (2)	0.32582 (8)	0.0259 (3)
C(7)	0.08782 (11)	1.06066 (18)	0.40054 (7)	0.0219 (3)
C(8)	0.30868 (12)	1.0154 (2)	0.39713 (10)	0.0320 (3)
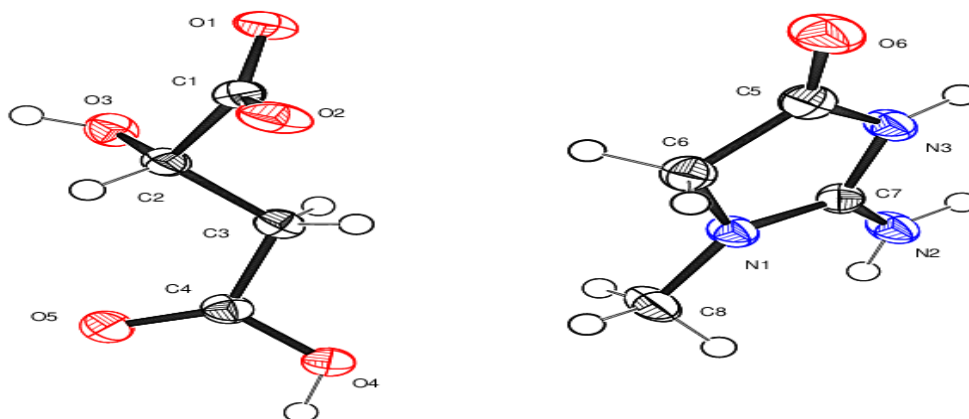
Figure 2
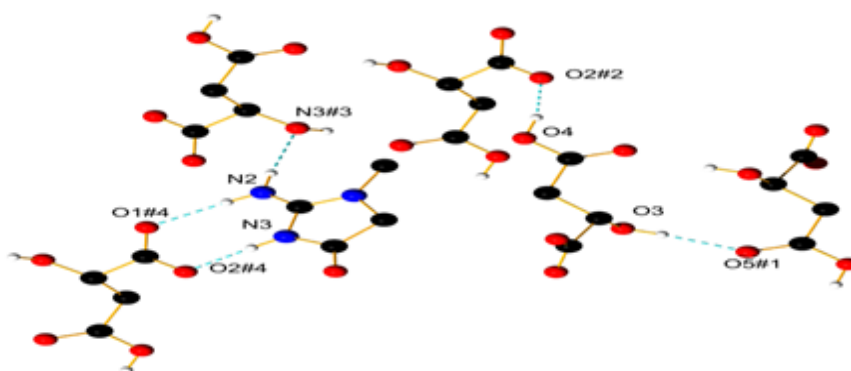
Figure 3
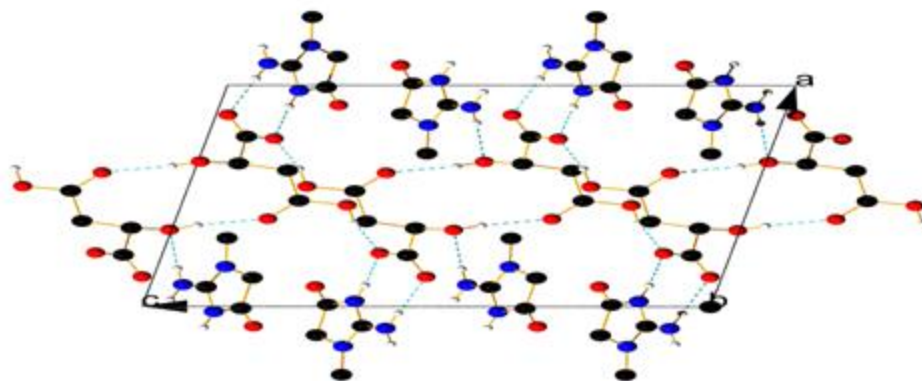
Figure 4

Table 3

D-H...A	d(D-H)	d(H...A)	d(D...A)	<(DHA)
O(3)-H(3)...O(5)#1	0.86(2)	1.94(2)	2.7766(13)	165.4(18)
O(4)-H(4)...O(2)#2	0.895(19)	1.659(19)	2.5385(12)	166.7(18)
N(2)-H(2A)...O(3)#3	0.881(17)	2.108(18)	2.9868(15)	176.0(15)
N(2)-H(2B)...O(1)#4	0.873(18)	1.987(18)	2.8558(14)	173.0(16)
N(3)-H(3A)...O(2)#4	0.884(17)	1.826(17)	2.7047(13)	172.1(16)

Symmetry transformations used to generate equivalent atoms: #1 -x+1,-y+2,-z   #2 -x+1,y+1/2,-z+1/2
#3 x,-y+5/2,z+1/2   #4 -x,y+1/2,-z+1/2

Powder X-ray diffraction analysis

Powder X-ray diffraction patterns were recorded using a Powder X-ray diffractometer (PXRD Rigaku Ultima III XRD) with CuKα, radiation (λ=1.5406Å) at room temperature. Finely crushed powder of creatininium malate was scanned in the 2θ values ranging from 10° to 60° and the XRD peaks recorded are indexed and shown in **(Figure 5)**. The XRD peaks of creatininium malate show the prominent (202) and (412) peaks. The sharp peaks and low full width half maximum (FWHM) values confirm good crystallanity of the grown crystal. The unit cell parameters determined from the single crystal XRD were used to index the hkl values of powder XRD peaks of creatininium malate.
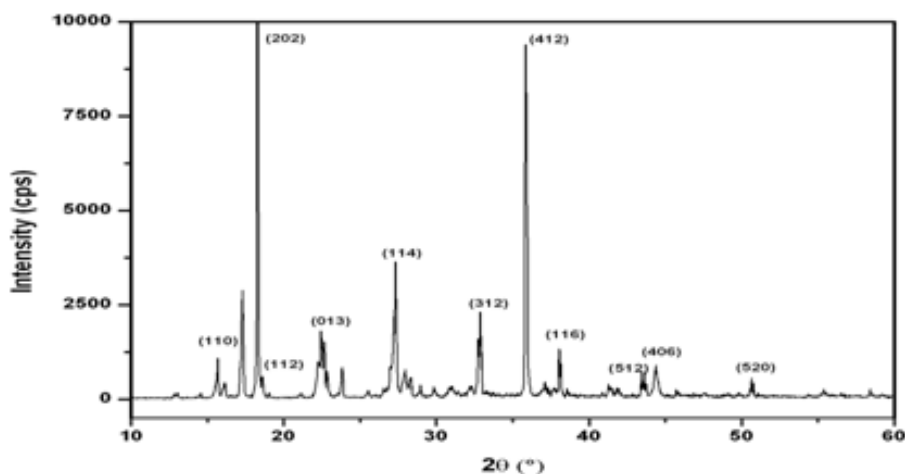
Figure 5

FTIR analysis

FTIR spectrum of creatininium malate was recorded using KBr pellet technique in the frequency range 400-4000 cm^{-1} and is shown in **(Figure 6)**. The strong band observed at 3398.7 cm^{-1} is due to O-H stretching vibration of COOH. The bands at 3270.4 cm^{-1} and 3044 cm^{-1} are due to asymmetric and symmetric stretching vibration of −NH$_2$, respectively [21]. The absorption at 2921cm^{-1} is assigned to C-H symmetric stretching vibration [33]. The signal for the carbonyl (C=O) group of malic (dicarboxylic) acid is observed at 1758 cm^{-1} [34]. The sharp band at 1710 cm^{-1} indicates the carbonyl (C=O) group of creatinine molecule [17, 18, 21]. The signals at 1599 cm^{-1} and 1407.1 cm^{-1} are

due to the presence of asymmetric and symmetric vibration of COO⁻ (carboxylate ion) in the creatininium malate [34]. The band at 1341.5 cm⁻¹ corresponds to the O-H in-plane bending of COOH. The vibration at 1192 cm⁻¹ corresponds to the CH in-plane deformation. The band at 1045 cm⁻¹ is due to the C-C-N asymmetric stretching vibration and the band at 779 cm⁻¹ is attributed to the aromatic C-H bending [33]. The observed vibrational frequencies and their frequency assignments are listed in the **(Table 4)**.
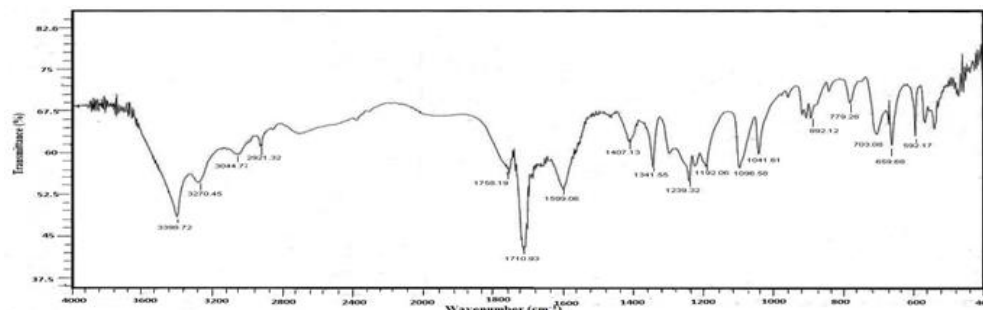

Figure 6

Table 4

Wavenumber (cm⁻¹)	Mode of vibration
3398	ν(O-H)
3270	ν_{asy}(N-H)
3044	ν_{sy} (N-H)
2921	$\nu_{sy}(CH)_3$
1758	ν(C=O) bonded
1710	ν(C=O)
1599	ν_{as}(COO)
1407	ν_{sy}(COO)
1341	δ(O-H)$_{in\ plane}$ of COOH
1239	ν(C-O-H)
1192	C-H inplane deformation
1096	ν_s(C-O), O-H
1041	C-C-N asym str, CH_2 wagging
892	ν_s(C-C-N)
779	Aromatic C-H bending
703	(NH2) out of plane δ
659	(COO)sci
592	δ(C-C=O)

Dielectric studies

Dielectric properties such as dielectric constant and dielectric loss of the grown creatininium malate crystal were studied as a function of frequency and temperature. The magnitude of dielectric constant depends on the degree of polarization charge displacement in the crystals. Two opposite faces of the sample were treated with good quality

silver paste in order to obtain good ohmic contact. Using the LCR meter the capacitance of the crystal was measured at different frequencies in the 50Hz – 1MHz range for various temperatures ranging from 30 to 90°C. The dielectric constant of the crystal was calculated using the relation

$$\varepsilon_r = C_{crys} / C_{air}$$

where C_{crys} is the capacitance of the crystal and C_{air} is the capacitance of air. **(Figure 7)** shows the variation of dielectric constant (ε_r) with log frequency. From the plot, it is observed that the dielectric constant increases in the lower frequency range and decreases with the increasing frequency in the temperature range of 30-90°C. The high dielectric constant at low frequency may be due to the contribution from all the four polarizations namely electronic, ionic, orientational and space charge polarization. At high frequencies the dielectric constant decreases as the space charge cannot keep up with the alternating field and hence the net polarization drops at high frequencies [35]. **(Figure 8)** shows the dielectric loss of the grown crystal as a function of frequency at different temperatures. It is observed from the figure that the dielectric loss follows the same trend as that of the dielectric constant. **(Figure 9)** shows the plot of temperature verses dielectric constant where dielectric constant increases with increase in temperature. This may be due to the fact that at high temperature the permanent dipoles acquire high mobility and can be more easily polarized which leads to the high dielectric constant [36]. Kim et al., reported that dielectric constant increases with increase in temperature for lithium tetraborate single crystal along [001] axis [37] and Das et al., also reported that dielectric constant of polycrystalline tungsten bronze electroceramics increases with increase in temperature [38].
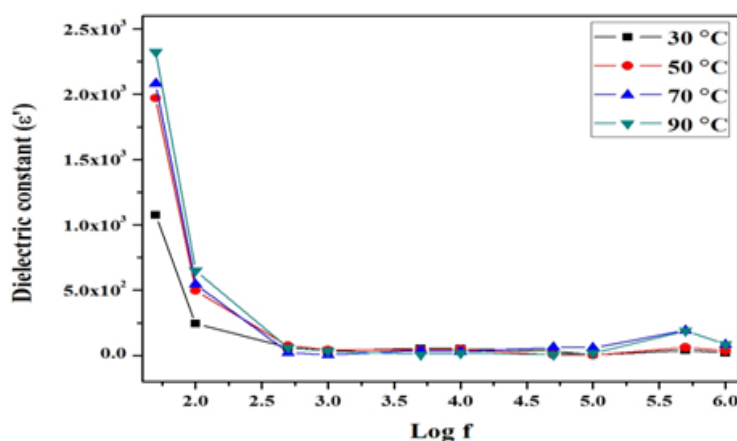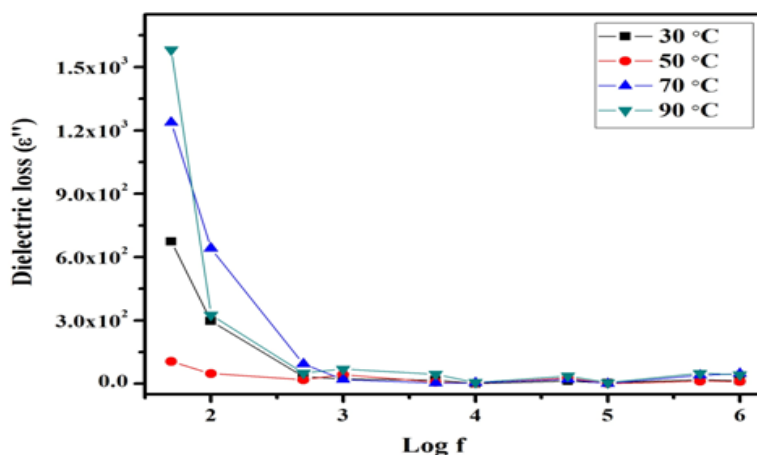

Figure 7

Figure 8

Thermal analysis

Thermal stability of the grown creatininium malate crystal was analyzed by thermo gravimetric and differential thermal analysis (TGA/DTA). **(Figure 10)** shows the TGA/DTA curve recorded for the creatininium malate crystal using thermal analyzer SDT Q600 V20.9 between 25°C and 300°C at a heating rate of 10 °C/min in nitrogen atmosphere. From TGA curve it is observed that the material is stable up to its melting point at 153.5° C, which confirms that there is no phase transition up to the melting point. Two weight losses observed at 176.8°C and 202.7°C are attributed to the decomposition of the material. The major weight loss occurs between 212.5°C and 275.5°C
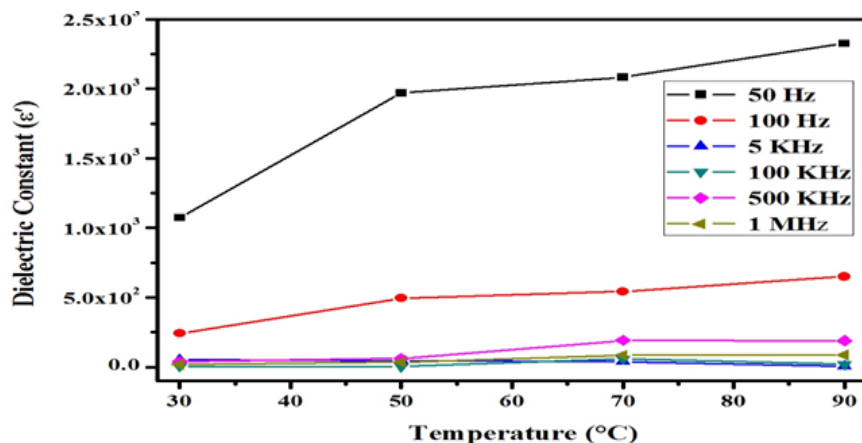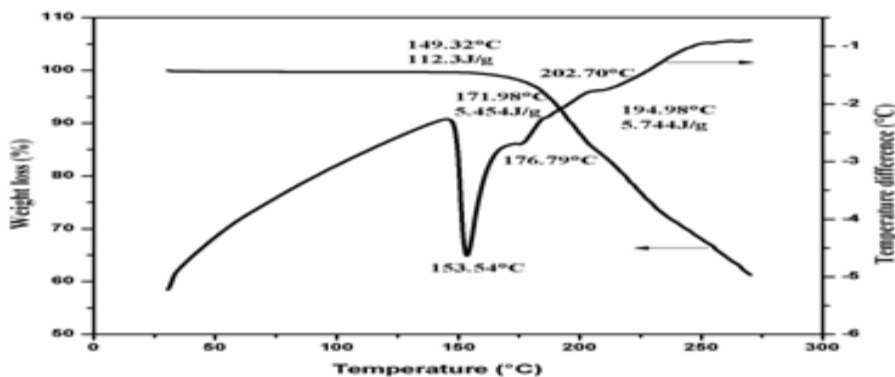

Figure 9

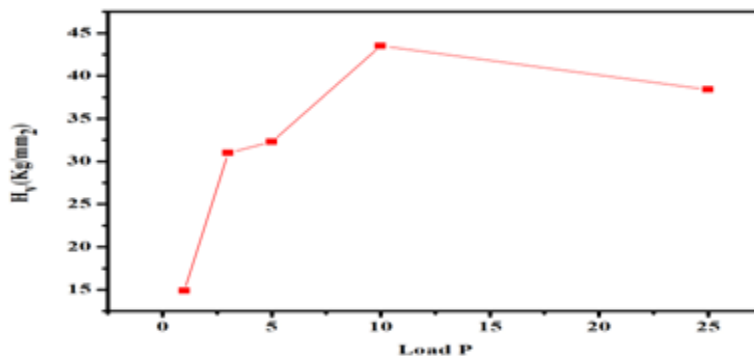**Figure 10**

Microhardness studies

Figure 11

Mechanical strength of the grown crystal can be studied by performing a microhardness test experiment. Practical hardness, an important solid state phenomenon, is the resistance offered by a material to localized plastic deformation caused by scratching or by indentation [39]. Vickers's micro hardness study was carried out using the Matsuzawa Hibiki model mmT X7 instrument. Selected smooth and flat surface of the grown crystal was subjected to the hardness study at room temperature in the load range 0 - 25g. The hardness of the crystal was measured from the applied load and the diagonal length of the indentations. For each load several indentations were made and the mean diagonal length was used for calculating the Vicker's hardness number (H_v) using the relation $H_v = 1.8544(P/d^2)$ Kg/mm^2 where P is the load applied in Kg and d is the mean diagonal length in millimeters. The plot drawn between the hardness values and corresponding loads is shown in **(Figure 11)**. It is observed from the figure that hardness (H_v) increases with increase in load up to 10g then it decreases. Cracks were formed after a load of 25g.

Conclusion

Creatininium malate, a novel single crystal, was synthesized and grown at room temperature using the slow evaporation method. Single crystal X-ray diffraction analysis reveals that the crystal belongs to monoclinic system with space group of P2$_1$/c. Presence of functional groups and hence the molecular structure is confirmed by FTIR analysis. Dielectric studies show that the dielectric constant of creatininium malate crystal increases at lower frequencies and decreases at higher frequencies due to various contribution of polarization mechanism. TGA and DTA reveal that the compound is stable at its melting point is ~153.5°C. Vickers microhardness value increases with increasing load and the work hardening coefficient reveals that creatininium malate belongs to category of soft materials. As there is no phase transition before the melting point attempts may be made to grow the creatininium malate single crystals from the melt technique.

Supplementary Data

Further information on the X-ray crystal structure data of compound (I) can be ordered from The Cambridge Crystallographica Data Center (E-mail: deposit@ccdc.cam.ac.uk) under the depository number CCDC 1004855.

Acknowledgements

References

[1]   Robert W Boyd, Nonlinear Optics, Third Edition, Elsevier, United States of America 2008.
[2]   Sreevalsa VG, Jayalekshmi S, J Cryst Growth 2011, 324, 172-176.
[3]   Bloembergen N, J Nonlin Opt Phys 1996, Mat 5, 1-7.
[4]   Lakshaman Perumal CK, Arulchakkaravarthi A, Rajesh NP, Santhaaraghavan P, Ramasamy P, Mater Lett 2002, 56, 578- 586.
[5]   Santhakumari R, Ramamurthi K, Vasuki G, Bohari MY, Bhagavannarayana G, Spectrochim Act A 2010, 76, 369-375.
[6]   Vijayan N, Ramesh Babu R, Gunasekaran M, Gopalakrishnan R, Ramasamy P, J Cryst Growth 2003, 256, 174-182.
[7]   Dixit VK, Vanishri S, Bhat HL, Gomes EDM, Belsley M, Santinha C, Arunmozhi G, Venkararamanan V, Proena F, Criado A, J Cryst Growth 2003, 253, 460-466.
[8]   Smith G, Pascoe CE, Kennard CHL, Byriel KA, Aust J Chem 1999, 54(1), 71-74.
[9]   Ueda H, J Chem Phys 1964, 40(3), 901-905.
[10] Smith G, White JM, Aust J Chem 2000, 54(2), 97-100.
[11] Moghimi A, Sharif MA, Aghabozorg H, Acta Cryst 2004, E60, o1790-o1792.
[12] Moghimi A, Khavassi HR, Dashestani F, Maddah B, Moradi S, J Iran Chem Soc 2007, 4(4), 418-430.

[13] Bahadur SA, Kannan RS, Sridhar B, Acta Cryst 2007, E63, o2387-o2389.
[14] Bahadur SA, Sivapragasam S, Kannan RS, Sridhar B, Acta Cryst 2007, E63, o1714-o1716.
[15] Ali AJ, Acta Cryst 2011, E67, o2905.
[16] Ali AJ, Acta Cryst 2011, E67, o1376.
[17] Mitewa M, Gencheva G, Bontchev PR, Angelova O, Polyhedran 1988, 7, 1273-1278.
[18] Muralidharan S, Nagaraja KS, Udupa MR, Polyhedran 1984, 3, 619-621.
[19] Bayrak C, Bayari SH, Hacettepe J Biol & Chem 2010, 38, 107-118.
[20] Panfil A, Fiol JJ, Sabat M, J Inorg Biochem 1995, 60, 109-122.
[21] Costa BSP, Baran EJ, Piro OE, Polyhedron 1997, 11, 3379-3383.
[22] Perpetuo GJ, Janczak J, Acta Cryst 2003, C59, o709-o711.
[23] Babu GA, Bhagavannarayana G, Ramasamy P, J Cryst Growth 2008, 310, 1228-1238.
[24] Balasubramaniam D, Sankar R, Shankar VS, Murugakoothan P, Arulmozhichelvan P, Jayavel R, J Mater Chem Phys 2008, 107, 57.
[25] Rajesh P, Ramasamy P, Kumar B, Bhagavanarayana G, Physica B 2010, 405, 2401-2406.
[26] Jaikumar D, Kalainathan S, Bhagavanarayana G, J Cryst Growth 2009, 312, 120-124.
[27] Bahadur SA, Sivapragasam S, Kannan RS, Sridhar B, Acta Cryst 2007, E63, o1714-o1716.
[28] Stoe, Cie, X-Area (Version 1.35) and X-RED32 (Version 1.31), Stoe, Cie Darmstadt, Germany, 2006.
[29] Sheldrick GM, SHELXS -97 and SHELXL-97, Programs for the solution and refinement of Crystal structures, University of Göttingen, Germany, 1997.
[30] Farrugia L J, J Appl Cryst 1997, 30, 565.
[31] Macrae CF, Bruno I J, Chisholm JA, Edgington PR, McCabe P, Pidcock E, Rodriguez-Monge L, Taylor R, Van de Streek J, Wood PA, J Appl Cryst 2008, 41, 466-470.
[32] Spek AL, Acta Cryst 2009, D65, 148 -155.
[33] Ali AJ, Thangarasu S, Athimoolam S, Sridhar B, Bahadur SA, J Arch Phy Res 2012, 3(5), 354-362.
[34] Mohan J, Organic Spectroscopy Principles and Applications, North America, 2000.
[35] Kittel C, Introduction to Solid State Physics, Eighth Edition, John Wiley & Sons, United States of America, 2005.
[36] Jindal UC, Material Science and Metallurgy, Dorling Kindersley, India, 2012.
[37] Kim CS, Jun BE, Baek HH, Kim DJ, J Korean Phys Soc 2003, 42, S1038-S1041.
[38] Das PR, Pati B, Sutar BC, Choudhury RNP, J Mod Phys 2012, 3, 870-880.
[39] Rajendran V, Materials Science, Tata Mc Graw-Hill, New Delhi, 2011.